PHYSICAL REVIEW E, VOLUME 64, 0664XX

Instability of a current-carrying finite-beta collisional plasma

E. Y. Choueiri
Electric Propulsion and Plasma Dynamics Laboratory, Princeton University, Princeton, New Jersey 08544
(Received 4 June 2001; revised manuscript received 20 August 2001)

The microinstability of a cross-field current-carrying plasma in which the electrons collisions are important on the time scale of the oscillations and can be modeled with a Bhatnagar-Gross-Krook operator is studied using linearized kinetic theory under conditions of finite electron beta. The finiteness of beta allows for coupling between electrostatic and electromagnetic modes and necessitates dealing with the entire dispersion tensor. Some additional fundamental features of the resulting instability are identified and contrasted with those found in previous studies of the lower hybrid current-driven instability in which either collisions or finite-beta effects were neglected. As beta increases, collisions play a more important role in destabilization, alter the character and extent of electromagnetic coupling, shift the instability to more perpendicular modes, and lead to a recapturing of some of the fluidlike properties the modes have in the electrostatic limit in contrast with their highly kinetic character in the collisionless limit.

DOI: 10.1103/PhysRevE.64.0664XX PACS number(s): 52.35.Qz, 52.75.Di

I. INTRODUCTION

The microinstabilities of a plasma carrying a cross-field current have been studied extensively due to their relevance to problems in space physics, controlled fusion, and some current-driven plasma devices. These instabilities typically produce lower hybrid waves that often play a significant role in altering transport processes. Kinetic descriptions of these instabilities where the effects of electron collisions are included, have been presented in the electrostatic limit [1–6] that is valid for low-beta plasmas. Studies of the effects of finite beta on such current-driven modes, which introduce the possibility of electromagnetic waves, have been made in the collisionless limit [7–21] and showed that a large enough beta can significantly alter the growth rates of these instabilities. Originally, the effects of finite beta were believed to be globally stabilizing [7–9]. The initial focus was on either perpendicular or nearly perpendicular propagation with respect to the magnetic field, typical of the modified two-stream instability, for which electromagnetic effects [which become important when the (current) drift velocity u_{de} exceeds the Alfvén velocity v_A] were found to be stabilizing.

The stability of a current-carrying plasma in which the effects of finite-beta *and* collisions are present together has not yet received much attention, probably because of the intuitive expectation that both effects would be stabilizing. However, considering the mathematically nonlinear interplay between these effects and the source of the instability (the current), it is conceivable that these effects may lead to both qualitative and quantitative changes to the nature of the instability, its growth rates, scaling, and angular dependencies. If indeed such effects can qualitatively alter the character of the previously known (electrostatic/collisional or electromagnetic/collisionless) unstable modes, it would be of fundamental importance to characterize the resulting modes and contrast them with previous knowledge. Aside from its fundamental value, the results of such a study would be useful in applications where the stability of a collisional finite-beta plasma is in question, such as, in some current-driven low-temperature plasma devices, and space physics problems.

In this paper we address the microstability of a plasma carrying a cross-field current in the presence of *both* electron collisions and finite-beta effects, discuss its fundamental features, and contrast them with those obtained in the electrostatic or collisionless limits. We are only concerned with modes driven by a cross-field (electron) current, represented by a drift velocity u_{de} and not by gradients in the plasma. Therefore, the applicability of the results extends to homogeneous plasmas, or inhomogeneous plasmas when either the current importance overwhelms that of the diamagnetic drifts resulting from the gradients or when the effects of the latter can also be represented to a first order by u_{de}. It is also relevant to mention that our focus is on the fundamental aspects of the instability and not on the application to specific plasmas or plasma devices, although the choice of the range of parameters for the calculations was done with some of these plasmas in mind.

We start with a description of the kinetic formalism behind the study and a discussion of the adopted collision operator. In Sec. III we discuss the effects of electron collisions on the electrostatic (zero beta) modes to provide connection with previous literature on the subject. In Sec. IV we describe in detail the electromagnetic effects resulting from the finiteness of beta. In particular we discuss the dependence of the character and polarization of the unstable modes and the dependencies of their properties on collisionality, beta, drift velocity and ion mass and their kinship to whistlers. We summarize the results in Sec. V in the form of a list of conclusions drawn from the study.

II. KINETIC FORMULATION

A. Dispersion tensor for a current-carrying finite-beta collisional plasma

When the plasma beta, defined as the sum of the ratios of thermal pressure to magnetic pressure for all the charged species,

$$\beta=\sum \beta_s\equiv\sum \frac{n_s k T_s}{B_0^2/2\mu_0}, \tag{1}$$

is large enough that electromagnetic (transverse) modes cannot be neglected, linear wave dispersion in a plasma is described by the general relation

$$\begin{pmatrix} R_{xx} & R_{xy} & R_{xz} \\ R_{yx} & R_{yy} & R_{yz} \\ R_{zx} & R_{xy} & R_{zz} \end{pmatrix} \begin{pmatrix} E_x^{(1)} \\ E_y^{(1)} \\ E_z^{(1)} \end{pmatrix} = 0, \tag{2}$$

where the superscript (1) denotes the first order harmonic part of the linearly perturbed quantities (in this case, the components of the electric field vector **E**). In the above equation, R_{ij} represent the elements of the *dispersion tensor* $\mathbf{R}(\omega,\mathbf{k})$ and are generally complex functions of the frequency ω and wave vector $\mathbf{k}$ of the oscillations as well as of all the plasma parameters of the problem. As usual the dispersion relation is obtained from

$$\det|R_{ij}(\omega,\mathbf{k})|=0. \tag{3}$$

An analog of Eq. (2) that offers the advantage of separating the effects of electromagnetic and electrostatic effects in the dispersion tensor [22] can be written in terms of the electrostatic potential Φ, defined by $-\nabla\Phi\equiv(\mathbf{E}+\partial\mathbf{A}/\partial t)$ and electromagnetic potential, **A**, defined by $\mathbf{B}=\nabla\times\mathbf{A}$ (where **B** is the magnetic field)

$$\begin{pmatrix} D_{11} & D_{12} & D_{13} \\ D_{21} & D_{22} & D_{23} \\ D_{31} & D_{32} & D_{33} \end{pmatrix} \begin{pmatrix} \Phi^{(1)} \\ A_x^{(1)} \\ A_z^{(1)} \end{pmatrix} = 0. \tag{4}$$

The corresponding dispersion relation is obtained from

$$\det|D_{ij}|=0. \tag{5}$$

The above matrix equation, dispersion relation, and the dispersion tensor elements D_{ij} are the analogs of Eqs. (2) and (3) and the tensor R_{ij}, respectively, in the potential formalism. Once explicit expressions for D_{ij} are obtained, the elements R_{ij} can be calculated through transformation relations derived from their definitions.

Starting with the Vlasov equation with a collision operator represented by the Bhatnagar-Gross-Krook (BGK) model [23] (which is discussed in Sec. II B)

$$\frac{\partial f_s}{\partial t}+\mathbf{v}\cdot\nabla\mathbf{x} f_s+\frac{q_s}{m_s}[\mathbf{E}(\mathbf{x},t)+\mathbf{v}\times\mathbf{B}]\cdot\nabla_{\mathbf{v}} f_s(\mathbf{x},\mathbf{v},t) = -\upsilon_s\left(f_s-\frac{n_s}{n_s^{(0)}}f_a^{(0)}\right), \tag{6}$$

the elements D_{ij} of the dispersion tensor can be derived. We have given an explicit derivation of these in Ref. [24] (for the case of a cross-field current) where we used them in the calculation of anomalous transport in current-driven plasma thrusters. Since the focus of that work was on the nonlinear effects only a cursory discussion of the linear modes was given.

From that work we quote the result

$$D_{11}=1+\alpha_i(1+\zeta_i Z_i)+\alpha_e\left(\frac{1+\zeta_{e0}e^{-\mu_e}\sum_{n=-\infty}^{\infty} I_n Z_{\mathrm{en}}}{1+i(\nu_e/k_z v_{\mathrm{te}})e^{-\mu_e}\sum_{n=-\infty}^{\infty} I_n Z_{\mathrm{en}}}\right), \tag{7}$$

$$D_{12}=-i\frac{\omega_{\mathrm{pe}}^2}{\tilde{\omega}^2}\frac{k_z}{k}\zeta_{e0}\sqrt{2\mu_e}e^{-\mu_e}\sum_{n=-\infty}^{\infty}(I_n-I_n')(1+\tilde{\zeta}_{e0}Z_{\mathrm{en}}), \tag{8}$$

$$D_{13}=2\frac{\omega_{\mathrm{pe}}^2}{\tilde{\omega}^2}\frac{k_z}{k}\zeta_{e0}e^{-\mu_e}\sum_{n=-\infty}^{\infty} I_n\left\{\vartheta_n^2 Z_{\mathrm{en}}+\left[\left(\frac{u_{\mathrm{de}}}{u_{\mathrm{te}}}\right)^2/\zeta_{e0}\right]+(1+\zeta_{\mathrm{en}}Z_{\mathrm{en}})\left(\vartheta_n\frac{k_\perp^2-k_z^2}{k_\perp k_z}-\zeta_{\mathrm{en}}\right)\right\}, \tag{9}$$

$$D_{22}=1-N^2+\frac{\omega_{\mathrm{pi}}^2}{\omega^2}\zeta_i Z_i+\frac{\omega_{\mathrm{pe}}^2}{\tilde{\omega}^2}\zeta_{e0}\mu_e e^{-\mu_e}\times\sum_{n=-\infty}^{\infty}\left[\frac{n^2}{\mu_e^2}I_n+2(I_n-I_n')\right]Z_{\mathrm{en}}, \tag{10}$$

$$D_{23}=-i\frac{\omega_{\mathrm{pe}}^2}{\tilde{\omega}^2}\zeta_{e0}\sqrt{2\mu_e}e^{-\mu_e}\sum_{n=-\infty}^{\infty}(I_n-I_n')\times\left[1+\left(\frac{k_z}{k_\perp}\vartheta_n+\zeta_{\mathrm{en}}\right)Z_{\mathrm{en}}\right], \tag{11}$$

$$D_{33}=1-N^2+\frac{\omega_{\mathrm{pi}}^2}{\omega^2}\zeta_i Z_i+2\frac{\omega_{\mathrm{pe}}^2}{\tilde{\omega}^2}\frac{k_\perp^2}{k^2}\left[\left(\zeta_{e0}-\frac{k_z}{k_\perp}\frac{v_{\mathrm{de}}}{v_{\mathrm{te}}}\right)^2+\zeta_{e0}e^{-\mu_e}\sum_{n=-\infty}^{\infty} I_n Z_{\mathrm{en}}\left(\frac{k_z}{k_\perp}\vartheta_n+\zeta_{\mathrm{en}}\right)^2\right], \tag{12}$$

$$D_{21}=-D_{12},\quad D_{31}=\frac{k_\perp^2}{k^2}D_{13}, \tag{13}$$

$$D_{32}=-\frac{k_\perp^2 2}{k^2}D_{23}, \tag{14}$$

where I_n is the modified Bessel function of the first kind of order n and where we have used the following definitions

$$\zeta_{\mathrm{en}}\equiv\frac{\omega+n\omega_{\mathrm{ce}}-k_\perp u_{\mathrm{de}}+i\nu_e}{k_z v_{\mathrm{te}}},\quad \zeta_i\equiv\frac{\omega-k_\perp u_f}{k v_{\mathrm{ti}}}, \tag{15}$$

$$\tilde{\omega} \equiv \omega + i\nu_e, \quad \tilde{\zeta}_{e0} \equiv \frac{\tilde{\omega}}{k_z v_{te}} = \zeta_{e0} + \frac{k_\perp}{k_z}\frac{u_{de}}{v_{te}}, \tag{16}$$

$$\vartheta_n \equiv \frac{k_z}{k_\perp}(\zeta_{en} - \tilde{\zeta}_{e0}), \quad Z_{en} \equiv Z(\zeta_{en}), \quad I_n \equiv I_n(\mu_e). \tag{17}$$

Here u_{de} is the electron drift velocity representing the current that is taken to be perpendicular to the magnetic field, Z is the standard plasma dispersion function, μ_s is

$$\mu_s \equiv \frac{r_{cs}^2 k_\perp^2}{2} \tag{18}$$

and the thermal velocity, plasma frequency and cyclotron frequency of species s are, respectively, given by their standard definitions

$$v_{ts} = (2T_s/m_s)^{1/2}, \quad \omega_{ps} \equiv \left(\frac{q_s^2 n_{0_s}}{\epsilon_0 m_s}\right)^{1/2}; \quad \omega_{cs} \equiv \frac{q_s B_0}{m_s}. \tag{19}$$

In Eq. (15), u_f represents the plasma velocity in the laboratory reference frame. In this paper we stay in the plasma flow rest frame and set $u_f = 0$. It is also useful to note that the refraction index N appearing in the above dispersion tensor can be related to the plasma parameters through the following relation:

$$N^2 \equiv \frac{c^2 k^2}{\omega^2} = 2\frac{\omega_{pi}^2}{\omega^2}\frac{\mu_e}{\beta_e}\frac{m_i}{m_e}\frac{k^2}{k_\perp^2}. \tag{20}$$

Finally, by writing

$$\frac{\omega_{pi}^2}{\omega^2} = \frac{\alpha_i}{2\zeta_i^2} \quad \text{and} \quad \frac{\omega_{pe}^2}{\omega^2} = \frac{k^2}{k_\perp^2}\frac{\alpha_e}{2\zeta_e^2}, \tag{21}$$

where

$$\alpha_s \equiv \frac{k_\perp^2 \omega_{ps}^2}{k^2 \omega_{cs}^2 \mu_s} = \frac{2\omega_{ps}^2}{k^2 v_{ts}^2} = \frac{1}{k^2 \lambda_{ds}^2}, \tag{22}$$

(λ_{ds} is the Debye length for species s) and by defining a nondimensional parameter Ψ, related to the propagation angle (with respect to **B**) θ scaled by the mass ratio

$$\Psi \equiv (m_e/m_i)^{1/2}\frac{k}{k_z} = \frac{(m_e/m_i)^{1/2}}{\cos\theta}, \tag{23}$$

it can be verified that the following set of seven dimensionless parameters (with $u_f = 0$)

$$\frac{T_i}{T_e}, \ \frac{u_{de}}{v_{ti}}, \ \Psi, \ \beta_e, \ \frac{\omega_{pe}}{\omega_{ce}}, \ \frac{m_i}{m_e}, \ \frac{\nu_e}{\omega_{th}}, \tag{24}$$

completely specify the problem such that, for a given real wave number, kr_{ce}, (where r_{ce} is the electron cyclotron radius) we seek the roots, ω/ω_{th} and γ/ω_{th} (representing the frequency and growth rate of the wave) of the dispersion relation in Eq. (5). In the above we have used for a characteristic frequency, as typical of current-driven instabilities, the lower hybrid frequency

$$\omega_{th}^2 \equiv \frac{\omega_{pi}^2}{1 + (\omega_{pe}/\omega_{ce})^2} \simeq (\omega_{ci}\omega_{ce})^{1/2}, \tag{25}$$

where the approximation holds when $\omega_{ce}\omega_{ci} \ll \omega_{pe}^2$. As also typical of such current-driven instabilities the ratio u_{de}/v_{ti} is particularly important as it controls the threshold and growth rate of the instability. Henceforth, we denote this ratio by U_{de}.

It is also worth mentioning that the *electrostatic* dispersion relation (obtained in the limit $\beta \to 0$) is simply $D_{11} = 0$. In that case it is convenient to divide the dispersion relation $D_{11} = 0$ by α_i and assume $\alpha_i \gg 1$. This will eliminate any explicit reference to m_i/m_e thus lowering the number of parameters to five, namely T_i/T_e, u_{de}/v_{ti}, Ψ, ω_{pe}/ω_{ce}, and v_e/ω_{th} while seeking the roots $\epsilon\omega/\omega_{th}$ and $\epsilon\gamma/\omega_{th}$ of the dispersion relation for a given ϵkr_{ce}, where the orthogonality factor is defined by

$$\epsilon \equiv \sin\theta = k_\perp/k. \tag{26}$$

Therefore, the dimensionless solutions are universal, i.e., independent of m_i/m_e. This universality is, unfortunately, lost in the electromagnetic case and all normalized solutions are generally heavy species specific. We shall primarily be concerned with argon although we will comment at the end of the paper on the extension of our results to other ion masses, specifically hydrogen, in order to provide a connection with the space physics literature. It is also relevant to note that for the cases discussed in this paper we have $\epsilon \simeq 1$ since it can be easily calculated that ϵ is close to unity when $\Psi \geqslant 0.005$ for argon and $\Psi \geqslant 0.05$ for hydrogen.

B. Collisional effects

We have chosen a collision model that was proposed in the classical paper of Bhatnagar, Gross, and Krook [23]. In that model the collision-induced loss rate of particles from an elemental phase space volume is represented by $-\nu_s f_s$ and the corresponding gain rate by $\nu_s f_{s0}$, where ν_s is the collision frequency of the s species. The validity of our results extends only to plasmas where this model is valid.

Since the collision frequency in the BGK model is not taken as an explicit function of the distribution function, the model is ignorant of the detailed collision dynamics and of any correlation between precollision and postcollision trajectories. Strictly speaking, the BGK collision model is only number density conserving and cannot conserve the energy and momentum as it does not include the macroscopic properties of the other species of the system. This becomes less problematic as the ionization fraction is decreased and most collisions happen with neutrals that form a stationary background. The BGK model is, therefore, best suited for large angle binary collisions, such as, those between charged and neutral particles. The model can, for example, describe the effects of electron collisions represented by ν_e if the

electron-neutral collision frequency ν_{en} dominates over the Coulomb collision frequency which, by definition, is the case in a weakly ionized plasma.

It can be shown [25], however, that for a current-carrying plasma the BGK model is momentum conserving if the electrons carry the bulk of the current, which is the case of many plasmas of interest, such as, in current-driven plasma thrusters [26]. The model can, under such conditions, represent the effects of electron-neutral, ion-neutral and electron-ion collisions.

The fact remains that the BGK model operator is not fundamentally inherent to kinetic theory and does neither represent the dependence of the collision frequency on the velocity nor does it account for the difference between the energy and momentum equilibration processes during a collision. The model has, however, been used with good success in studying some features of current-driven instabilities in the ionosphere (see the citations in Sec. I). Its limitations and applicabilities have been discussed elsewhere [27,28] in that context along with amendments to extend its validity.

For our study we consider the case where the ions are collisionless on the characteristic time scale of the unstable modes that, as we shall see, is the inverse of the lower hybrid frequency. This is the case for many plasmas of interest including those in current-driven plasma thrusters [24,29–31].

The electron collisions, on the other hand, are introduced to the analysis through ν_e, which, in light of the comments above, can be taken to represent electron-neutral collisions, if the ionization degree is low, and Coulomb collisions, if such collisions happen to dominate.

III. EFFECTS OF COLLISIONS ON ELECTROSTATIC MODES

We start our numerical investigation by considering the effects of collisions on pure electrostatic modes. The resulting dispersion relation is $D_{11}=0$. In order to simplify the discussion we divide D_{11} by α_i and take $\alpha_i \gg 1$. We study the effects of finite-electron collision rate on the *dominant* modes by growth maximizing the solutions first over wave number then over propagation angle. The results of these calculations are shown in Figs. 1 and 2 for the case of an equithermal plasma ($T_i/T_e=1$) with U_{de} as a varying parameter. In order to show the effects of collisions we show the results of the collisionless case along with those obtained for a normalized electron collision frequency $\epsilon\nu_e/\omega_{lh}$ of unity.

It can be seen from Fig. 1 that, for a fixed current velocity, the growth-maximized temporal growth rates agree with those of collisionless theory as the propagation becomes more oblique with respect to the magnetic field (i.e., Ψ decreases). This is because oblique unstable lower hybrid waves have phase velocities on the order of the ion thermal velocity and are not in phase with the current. This means that electron scattering through collisions is not an important factor in the stability of these waves. As the waves become more perpendicular to the magnetic field, the electrons behave as if they had an effective mass $\overline{m_e}$, that is comparable or larger than the ion mass with [8]

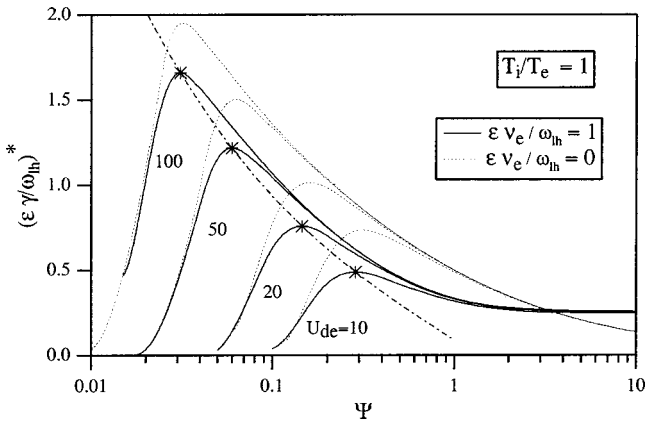

FIG. 1. Growth rate growth maximized over wavelength as a function of the normalized propagation angle Ψ with the dimensionless current velocity U_{de} as parameter and with the electron collision frequency set near the lower hybrid frequency. The asterisks denote the dominant modes (i.e., growth maximized over wavelength and Ψ).

$$\overline{m_e}=\Psi^2 m_i . \tag{27}$$

The dissipative effects of electron collisions become more important to the instability as the propagation angle increases. This is reflected by the decrease in growth rates γ^* in Fig. 1, over those of the collisionless case, with increasing Ψ. These growth rates are still, generally, on the order of ω_{lh}.

As Ψ increases further, an interesting reversal in the role of electron collisions from a stabilizing one to a destabilizing one occurs, reminiscent of the so-called ''Farley-Buneman instability'' [1,32–35] in which collisions play a destabilizing role. This reversal occurs at $\Psi=\Psi_r\approx 3.5$ for the case of the equithermal plasma with $\epsilon\nu_e/\omega_{lh}=1$. This destabilizing role of collisions is not important for the truly dominant unstable modes, i.e., those doubly maximized (over wavelength and Ψ) and marked by asterisks on the curves in the plots, but for low enough values of U_{de} it causes the most perpendicular modes to attain growth rates approaching those of the dominant modes.

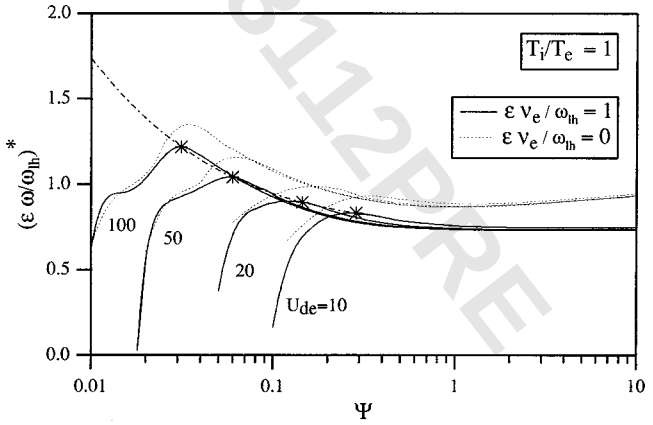

FIG. 2. Frequency growth maximized over wavelength as a function of the normalized propagation angle Ψ. Same conditions as in Fig. 1. The asterisks denote the dominant modes.

The effects of collisions on the growth-maximized wave frequency are shown in Fig. 2, where it can be seen that ω^* is slightly lower than in the collisionless case. The doubly maximized wave frequencies, denoted by an asterisk on that plot, are all near $\omega_{\rm lh}$ for the considered range of $U_{\rm de}$, thus extending the validity of the appellation ''lower hybrid current-driven instability'' (LHCDI) to the collisional regime.

The growth-maximized normalized wave number was found to become very close to its collisionless counterpart away from the fluid limit as $U_{\rm de}$ is increased. In the fluid limit, reached with increasing Ψ, the asymptotic values of $\epsilon k^* r_{\rm ce}$ are larger than those in the collisionless case.

The quantity $|\tilde{\zeta}_e|^*$ was found to attain larger values with increasing Ψ when collisions are present than it does under collisionless conditions. Physically, this supports the intuitive idea that collisions aid in approaching fluid conditions. Although the instability quickly becomes a fluid mode with increasing Ψ, the *dominant* mode (doubly maximized over wavelength and propagation angle) stays kinetic. Indeed, we can deduce from these calculations that the dominant mode is conditioned by a simple resonance relation, $|\tilde{\zeta}_e|^{**} \simeq 3$, (where the double asterisks refer to a doubly growth-maximized quantity) which is valid for the entire investigated region of parameter space.

Finally, it is clear from these results that the effects of collisions on the growth rates, frequencies, wave numbers, and thus phase velocities of the dominant modes are not pronounced and do not lead to a change in the character of these modes (i.e., large shifts in wavelength, or propagation angles).

IV. ELECTROMAGNETIC EFFECTS

Many kinetic studies of plasma instabilities use the electrostatic approximation, $\mathbf{k}\times\mathbf{E}^{(1)}\simeq 0$, which allows the use of an electrostatic potential to describe the perturbations. This can be attributed to the fact that at low thermal pressures (i.e., low β) electromagnetic modes can only contribute positive energy increments to the total perturbation energy and are, therefore, incapable of destabilizing the system [36]. A more detailed description of the role of finite beta in scaling electromagnetic effects is given in Sec. IV D below. For an infinite homogeneous plasma, it is known [22] that coupling between longitudinal and transverse oscillations leads to a sharing of the free energy between the two modes, which is consequently manifested in a reduction of the growth rates. This extent to which this coupling scales and is altered by collisional effects is our prime focus.

A. Polarization

Once a root of Eq. (5) is found, the corresponding components of the oscillating electric field can be found by solving Eq. (4) for $\Phi^{(1)}$, $A_x^{(1)}$, and $A_z^{(1)}$ then calculating the components of $\mathbf{E}^{(1)}$ from $\mathbf{E}^{(1)}=i\omega\mathbf{A}^{(1)}-i\mathbf{k}\Phi^{(1)}$ by eliminating $A_y^{(1)}$ with

$$A_y^{(1)}=-\frac{k_z}{k_\perp}A_z^{(1)}, \tag{28}$$

which results from the Coulomb gauge and the orientation of the wave vector, to get

$$E_x^{(1)}=i\omega A_x^{(1)}, \tag{29}$$

$$E_y^{(1)}=-ik_\perp\Phi^{(1)}-i\omega\frac{k_z}{k_\perp}A_z^{(1)}, \tag{30}$$

$$E_z^{(1)}=-ik_z\Phi^{(1)}+i\omega A_z^{(1)}. \tag{31}$$

The components of the oscillating electric field can, therefore, be directly obtained through the following transformation:

$$\begin{pmatrix} E_x^{(1)} \\ E_y^{(1)} \\ E_z^{(1)} \end{pmatrix} = i\omega \begin{pmatrix} 0 & 1 & 0 \\ -\frac{k_\perp}{k} & 0 & -\frac{k_z}{k_\perp} \\ -\frac{k_z}{k} & 0 & 1 \end{pmatrix} \begin{pmatrix} \frac{k}{\omega}\Phi^{(1)} \\ A_x^{(1)} \\ A_z^{(1)} \end{pmatrix}. \tag{32}$$

The electrostatic (or longitudinal) component, $E_s^{(1)}$ of the oscillating electric field, is by definition aligned with the wave vector and can therefore be found from

$$E_s^{(1)}=\frac{\mathbf{k}\cdot\mathbf{E}^{(1)}}{k}=\frac{k_\perp}{k}E_y^{(1)}+\frac{k_z}{k}E_z^{(1)}, \tag{33}$$

while the electromagnetic (or transverse) component $E_m^{(1)}$ is given by

$$E_m^{(1)}=(E^{(1)^2}-E_s^{(1)^2})^{1/2}. \tag{34}$$

Knowing the electrostatic and electromagnetic components we can calculate the following two ratios:

$$\frac{(\text{electrostatic field energy density})}{(\text{transverse field energy density})}=\frac{|E_s^{(1)}|^2}{|E_m^{(1)}|^2}, \tag{35}$$

$$\frac{(\text{electrostatic field energy density})}{(\text{magnetic field energy density})}=\frac{|E_s^{(1)}|^2}{|B^{(1)}|^2}=\frac{|\omega|^2}{k^2c^2}\frac{|E_s^{(1)}|^2}{|E_m^{(1)}|^2}, \tag{36}$$

where the last equality follows from Maxwell's linearized curl of $\mathbf{E}$ equation, $\mathbf{k}\times\mathbf{E}^{(1)}=\omega\mathbf{B}^{(1)}$, and the definitions

$$(\text{electric field energy density})\equiv\epsilon_0\frac{|E^{(1)}|^2}{2}, \tag{37}$$

$$(\text{magnetic field energy density}) \equiv \frac{|B^{(1)}|^2}{2\mu_0}. \qquad (38)$$

The ratios in Eqs. (35) and (36) will offer us insight into the polarization of the excited modes.

B. Numerical considerations

The calculations presented below are made using the entire dispersion tensor, Eqs. (7)–(14) and retaining the cyclotron harmonics. This has been shown to be necessary by Tsai *et al.* [19] who found that, in general, the terms associated with the cyclotron harmonics $n=\pm 1$ are required for a qualitatively correct representation of the kinetic cross-field instability. Their calculations also showed that terms with $|n|\geqslant 2$ typically result in a correction of the order of 20%. We have found that, for the range of parameters covered in our investigation, cyclotron summations with the seven terms, $n=0,\ \pm 1,\ \pm 2,\ \pm 3$ are enough to reduce the error below 2%.

C. Defining the parameter-space

Since, as mentioned in Sec. II A, the parameters for the electromagnetic problem are seven (excluding $\epsilon k r_{ce}$) T_i/T_e, u_{de}/v_{ti}, Ψ, β_e, ω_{pe}/ω_{ce}, m_i/m_e, and ν_e/ω_{lh}, we shall fix some of them and vary the others in order to have a manageable study of the new effects brought about by the electromagnetic parts of the dispersion tensor.

Specifically, we consider the case of an equithermal plasma by setting $T_i/T_e=1$. Furthermore, calculations show that the results become quite insensitive to ω_{pe}/ω_{ce} as long as it is much larger than unity. Physically, this is due to the fact that this parameter represents the scaling of the wavelength with respect to the Debye length as can be seen from Eq. (22) and since for the electrostatic problem the wavelengths were characterized by $\epsilon k \leqslant r_{ce}$ for the dominant modes, the shielding effects were not central to the problem when $\omega_{pe}\omega_{ce}\gg 1$. Since we do not know, *a priori*, the exact range of wavenumbers, we shall not set ω_{pe}/ω_{ce} at infinity but choose to set it at 100, typical of the plasma of a current-driven plasma thruster [29,30]. We shall set the parameter ν_e/ω_{lh} to unity in order to represent the effects of collisions when their frequency is on the same order as the expected oscillation frequency. In order to appreciate the effects of collisions we shall also present, for the sake of reference, some solutions for the collisionless plasma. The loss of universality mentioned at the end in Sec. II A forces us to fix the ion to electron mass ratio. We set the mass ratio m_i/m_e to that of argon, since many plasma thruster experiments [29,30] are conducted with that gas. As already mentioned, we shall comment in Sec. IV D 7 on the extension of the results to other ion masses in order to provide some degree of extrapolation to operation with other working fluids in plasma thrusters or to magnetospheric and astrophysical problems. Finally, the quantities u_{de}/v_{ti}, Ψ, and β_e will be varied parametrically to reveal the dominant modes.

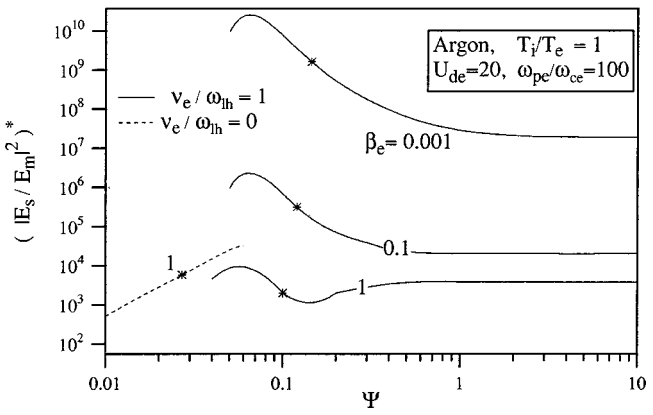

FIG. 3. Polarization of collisional and collisionless unstable modes in argon as a function of the normalized propagation angle and β_e. The solutions are growth maximized over the wavelength. The asterisks denote the dominant modes.

D. Results

1. The role of plasma beta in polarization

The importance of the plasma beta[1] as a scaling parameter for the polarization of the unstable oscillations can be seen from the curves of Fig. 3, which correspond to solutions growth maximized over wavelength. By varying β_e from 0.001 to unity, the ratio of electrostatic to electromagnetic energy density of the unstable waves drops by seven orders of magnitude indicating substantial electromagnetic polarization with increasing β_e.

The scaling of $|E_s^{(1)}|^2/|B^{(1)}|^2$ with β_e was found to have the same character as that for the curves discussed above; however, its magnitude is always below unity for the same parameters. This is a characteristic of the LHCDI which, like other cross-field current instabilities, has most of its energy in the fluctuating magnetic field because of its low phase velocity ([37], pp. 56–58) as can be seen from Eq. (36). Raising β_e to unity drops $|E_s^{(1)}|^2/|B^{(1)}|^2$ by more than three orders of magnitude indicating a sizable enhancement in magnetic field fluctuations.

Collisional effects on polarization. To the same figures discussed above, we have added solutions for the case of a collisionless plasma with $\beta_e=1$ to provide a link with previous studies [17,19]. As reported in these studies, where only collisionless plasmas were treated, the polarization of the unstable waves, at constant β_e, becomes monotonically more electrostatic as the propagation becomes more perpendicular. This is clearly not the case in the presence of collisions as can be seen from the present figures. Furthermore, since the shape of the curves in these figures is the same as those of the normalized wave number shown in Fig. 4, the energy deposited in the fluctuating magnetic field comes primarily from the long wavelength part of the unstable spectrum. This point may be of relevance to the problem of de-

[1]Since, $\beta=\beta_e(1+T_i/T_e)$ and we are specifying the ion to electron temperature ratio, scaling with the plasma beta is equivalent to scaling with the electron beta.

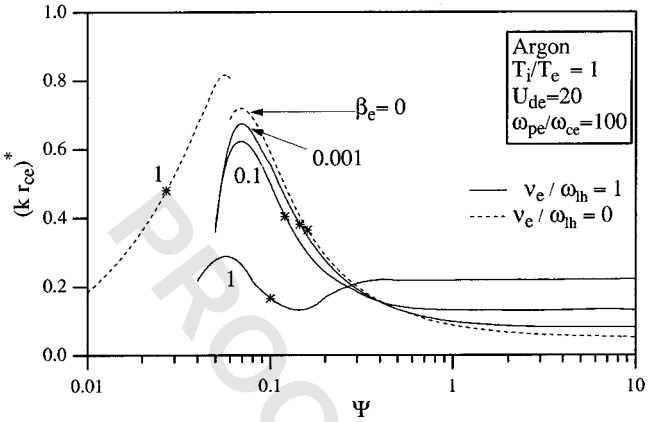

FIG. 4. Wavenumber of collisional and collisionless unstable modes in argon as a function of the normalized propagation angle and β_e. Same conditions as in Fig. 5. The asterisks denote the dominant modes.

veloping turbulence suppression schemes in plasma devices where such an instability is at play.

In studying the figures in this section it is useful to keep in mind that the $\beta_e=0.001$ solutions are practically coincidental with the electrostatic solutions shown in Fig. 1 (with the obvious exception of the curves representing polarization quantities, which have no equivalent in the purely electrostatic problem). We shall, therefore, refer to the $\beta_e=0.001$ solutions whenever we are comparing finite-β_e solutions to purely electrostatic ones.

2. Growth rates of mixed polarization modes

As we reported briefly in Ref. [24], the enhancement of electromagnetic coupling with increasing β_e results in a damping of the dominant mode. As seen in Fig. 5 the damping is not drastic since more than a three order of magnitude increase in β_e corresponds to only a factor of 2 decrease in the growth rate of the dominant modes. The instability not only persists under finite-β_e effects but, as can be seen from the $\beta_e=1$ (and $\nu_e/\omega_{lh}=1$) curve in that figure, also encompasses a somewhat wider range of propagation angles than it did for the purely electrostatic case.

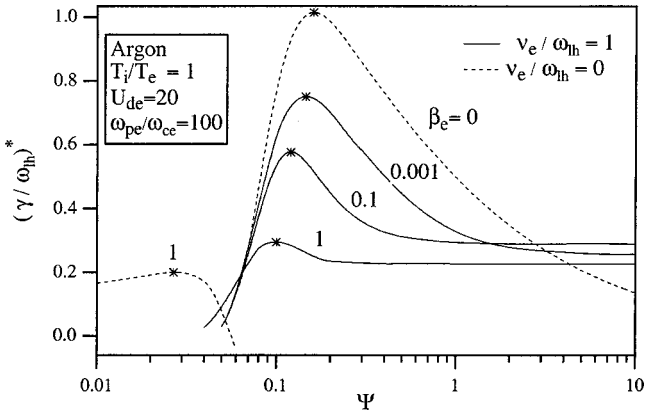

FIG. 5. Growth rates of collisional and collisionless unstable modes in argon as a function of the normalized propagation angle and β_e. Same conditions as in Fig. 5. The asterisks denote the dominant modes.

The finite-β_e effects, therefore, are *not* globally stabilizing as was previously thought [6–9], even for drift velocities exceeding the Alfvén velocity, but rather result in the excitation of finite growth modes with mixed polarization. This extends the validity of the findings reported in Refs. [37, 13,17]] to the collisional case.

The collisionless solutions are also shown in Fig. 5 for both the $\beta_e=0$ (electrostatic) and $\beta_e=1$ cases. It is obvious that the effects of finite β_e are qualitatively different for the collisionless and collisional dominated cases.

In the absence of collisions the electromagnetic effects result in a shifting of the instability to more oblique propagation with respect to the magnetic field. For argon with $\beta_e=1$ and $U_{\rm de}=20$ for instance, the dominant mode shifts by more than 6 deg towards the magnetic field vector from the orientation of the purely electrostatic dominant mode. The shift is more pronounced for lighter atoms (approaching 50 deg for hydrogen). This effect was first discovered by Wu *et al.* [17] who noted that electromagnetic effects actually stabilize nearly perpendicular waves and destabilize more oblique ones. Since many of the preceding studies that addressed the finite-β_e effects on the electrostatic modified two-stream instability focused on either perpendicular or nearly perpendicular propagation, electromagnetic effects (which become important when $u_{\rm de}>v_A$) were generally thought to be stabilizing.

Collisional effects on growth rates. When electron collisions start to dominate, the instability changes considerably in character as it reverts to more perpendicular propagation. Indeed, the dependence of its growth rates on the propagation angle resembles more that of the electrostatic modes than that of the collisionless finite-β_e modes as can be learned from comparing the two $\beta_e=1$ curves in Fig. 5. This is a clear indication that, as the electromagnetic character of the waves prevails, the role of electron collisions in destabilization becomes quite important.

At $\beta_e=1$, for instance, electron collisions revert from a damping role to a destabilizing one when $\Psi=\Psi_r\simeq 0.05$ (intersection of the two $\beta_e=1$ curves) in contrast with a $\Psi_r \simeq 3.5$ for the electrostatic case (intersection of the $\beta_e=0.001$ curve and that corresponding to the $\nu_e=0$, $\beta_e=0$ conditions). Aside from shifting the instability to more perpendicular propagation, electron collisions can actually increase, albeit modestly, the growth rate of the *dominant* mode as can be seen from the maxima of the two $\beta_e=1$ curves. This is contrary to the effect electron collisions have on the dominant electrostatic modes studied in Sec. II B (see Fig. 1).

It is interesting to note that although electron collisions can greatly affect the growth rates of the finite-β_e unstable waves they have a relatively small effect on the extent of their polarization (i.e., on the *magnitude* of the ratios $|E_s^{(1)}|^2/|E_m^{(1)}|^2$ and $|E_s^{(1)}|^2/|B^{(1)}|^2$) and even less of an effect on the extent of polarization of the dominant modes (as can be seen from the location of the asterisks on the $\beta_e=1$ curves of Fig. 3).

3. Phase velocities

The phase velocities of the unstable waves (growth-maximized over wavelength) under collisional conditions were found to range between one and ten times the ion thermal velocity. The phase velocities of the *dominant modes* for all the studied cases are about twice the ion thermal velocity. This insensitivity of the dominant mode phase velocity to the various parameters of the problem is indicative of the prevalence of a strong resonance condition.

4. Kinetic nature of instability

Resilient resonance conditions, such as, the one mentioned above, are symptomatic of kinetic instabilities. Our calculations show that, for the electromagnetic collisionless case ($\beta_e=1,\nu_e=0$), all the unstable waves (growth maximized over wavelength) have

$$|\zeta_i|^* \sim O(1) \quad \text{and} \quad |\zeta_{e0}|^* \leqslant 1, \tag{39}$$

which is indicative of the kinetic character of the instability when electromagnetic effects dominate in the absence of collisions. This result was first noted by Wu *et al.* [17] and later supported by the more accurate calculations of Tsai *et al.* [19] who included, as we did, the effects of finite cyclotron harmonics. The magnitudes of the above two quantities are such that the large and small argument expansions of the dispersion function, sometimes adopted to simplify plasma wave analysis, cannot be justified here. This fact combined with the pronounced electromagnetic nature of the instability renders the dispersion tensor too complicated for any incisive analytical treatment.

We can, therefore, conclude that the electrons are broadly resonant with the unstable waves while the resonance of the ions with the waves narrows with increasing electron collisionality (see below) and/or increasing electromagnetic effects (increasing β_e). This feature of the instability was exploited in our discussion of resonance broadening effects on the saturation of the instability in Ref. [24].

Collisional effects on the kinetic nature of the instability. Our calculations also showed that, quite unlike the electromagnetic collisionless case treated in the above mentioned works, the instability, as far as the electrons are concerned, quickly becomes nonresonant as the propagation becomes more perpendicular ($\Psi>1$). This was found to result from to the scattering role of collisions and not from any electromagnetic coupling effects. While it is possible to treat the electrons as a fluid for nearly perpendicular waves, the ions become strongly more resonant when electromagnetic effects become important.

We conclude from the above discussion that the highly kinetic nature of the mixed polarization instability, in question here, is somewhat weakened by electron collisions for the more perpendicular modes but is preserved for the dominant modes.

In sum, the role of collisions amounts to a recapturing of some of the fluidlike properties the modes had in the electrostatic limit in contrast with the highly kinetic character taken on by the instability in the collisionless limit (when finite-β_e effects are present) where it has been called ''kinetic cross-field streaming instability'' by previous authors [17].

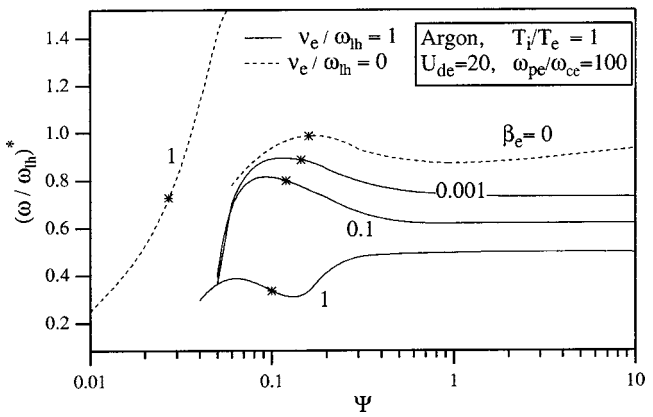

FIG. 6. Normalized frequencies for collisional and collisionless unstable modes in argon as a function of the normalized propagation angle and β_e. Same conditions as in Fig. 5. The asterisks denote the dominant modes.

5. Frequencies of the unstable modes and relation to whistlers

The frequencies of the unstable modes, growth maximized over wavelength, are shown in Fig. 6 where, consistent with the above results, we find that the angular dependence of the frequencies of the collisional mixed polarization modes resembles more that of the electrostatic collisionless modes than that of the collisionless mixed polarization modes. This indicates that unstable electrostatic oscillations couple differently with electromagnetic oscillations when collisions are important.

The question of which electromagnetic wave is being coupled to, in such finite-beta cross-field electron-ion streaming instabilities, was first addressed by Ross [38] who found that, in either the ''adiabatic'' limit, $|\zeta_{e0}|\ll 1$, or the fluid limit, $|\zeta_{e0}|\gg 1$, the unstable mode was essentially a whistler wave excited by the current (ion beam in the electron frame). Wu *et al.* [17] and Tsai *et al.* [19] also found that many of the dependences of the unstable kinetic modes can, indeed, be gleaned from a generalized finite-beta description of whistlers.

We shall, therefore, use the well-known dispersion relation for oblique whistlers [39,40],

$$\omega_w = \frac{c^2k^2}{\omega_{pe}^2}\,\omega_{ce}\cos\theta, \tag{40}$$

in a general assessment of the kinship between our *collisionally dominated* unstable oscillations and the whistler mode. Since Eq. (40) does not take into account kinetic and collisional effects we shall not expect a very accurate description of this kinship.

For this purpose, we restrict our discussion to the real part of the frequency and use

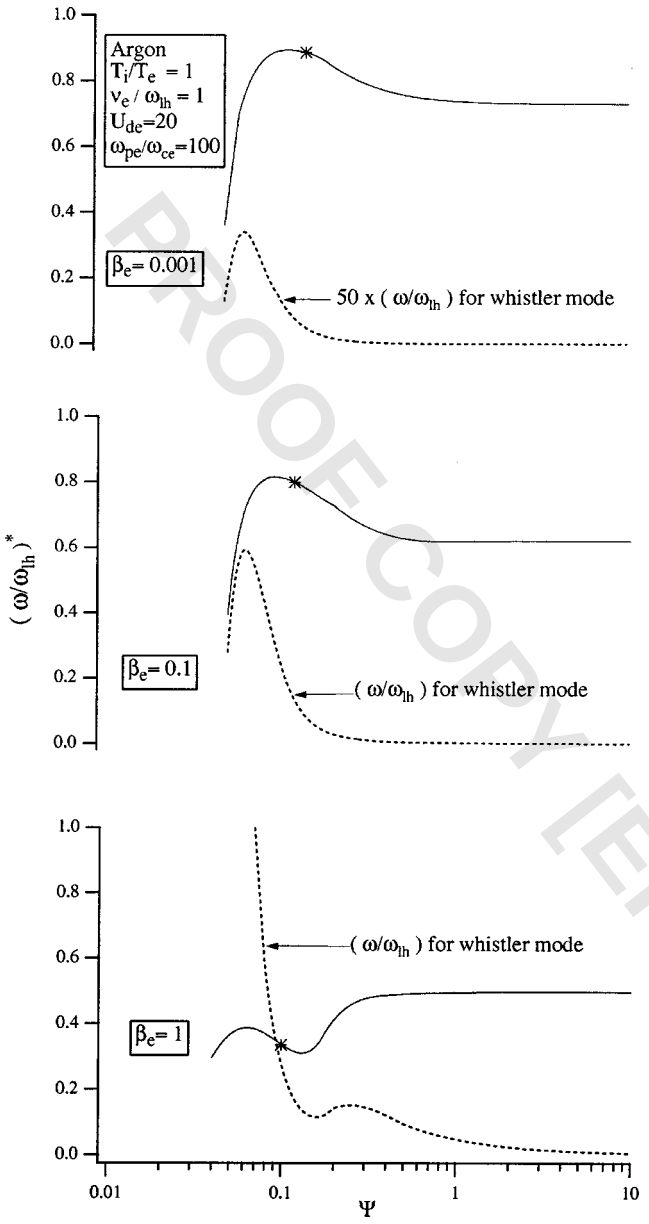

FIG. 7. Normalized frequencies of Fig. 6 compared with those obtained from Eq. (42) for collisional unstable modes in argon plotted as a function of the normalized propagation angle and β_e. The solutions are growth maximized over the wavelength. The asterisks denote the dominant modes.

$$\frac{ck}{\omega_{pe}} = kr_{ce}\left(\beta_e \frac{T_i}{T_e}\right)^{1/2} \tag{41}$$

to rewrite Eq. (40) as a function of the problem's independent parameters

$$\frac{\omega_w}{\omega_{lh}} = (kr_{ce})^2 \frac{T_i}{T_e}\frac{\beta_e}{\Psi}. \tag{42}$$

We have evaluated ω_w/ω_{lh} using the kr_{ce} versus Ψ growth-maximized solutions plotted in Fig. 4 and plotted the resulting normalized frequency versus Ψ in Fig. 7 for three values of β_e. It is evident from the top plot that, near the electrostatic limit ($\beta_e = 0.001$), Eq. (42) describes the frequency dependence but not its magnitude. When β_e is increased by two orders of magnitude, thus enhancing the coupling with electromagnetic modes, the middle plot of the same figure shows that the frequencies obtained from Eq. (42) coincide with those of the most oblique unstable waves. If β_e is further increased to unity, we see from the bottom plot that the only mode whose frequency coincides with that obtained from Eq. (42) is the dominant one.

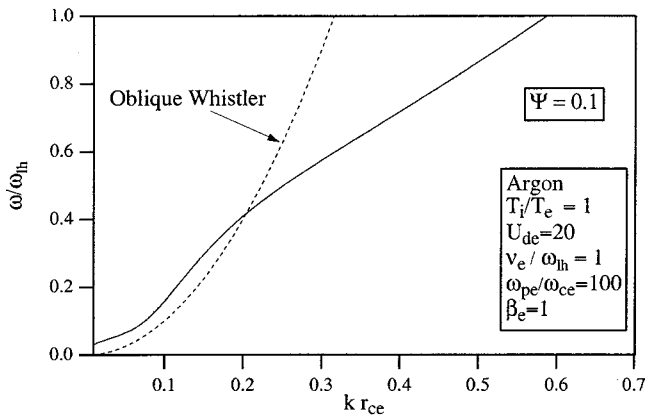

FIG. 8. Dispersion relation of oblique whistlers [Eq. (42)] compared to that computed for the parameters corresponding to the dominant mode of the bottom plot of Fig. 7.

In order to better see the connection with the whistler mode at these conditions, we need to compare the actual dispersion relation at a fixed propagation angle over a range of wave numbers. In Fig. 8 we compare the dispersion relation of oblique whistlers [Eq. (42)] to that computed for the parameters corresponding to the dominant mode of the bottom plot of Fig. 7. We find that the computed dispersion relation exhibits a change in curvature such that for a range of long wavelengths the rise in frequency follows the quadratic law of Eq. (42) implying that the phase velocity increases with the frequency ($\sim\sqrt{\omega}$) like the whistler. As the wavelength decreases, the computed dispersion relation changes in curvature resulting in a decrease of the phase velocity with the frequency and a departure from the classical oblique whistler relation. The coupling with the classical whistler wave is, therefore, most evident at longer wavelengths consistent with our previous finding that the energy deposited in the magnetic field (and hence electromagnetic polarization) comes primarily from that part of the unstable spectrum.

6. Effects of the drift velocity

In order to study the effects of the drift velocity on the instability, we have computed the complete set of solutions for four values of $U_{de} \equiv v_{de}/v_{ti}$, typical of the plasma in current-driven plasma thrusters [29,30], namely, $U_{de} = 10$, 20, 50, and 100. The growth rates are shown in Fig. 9. It is evident that the magnitude of the growth rates at and near the conditions for the dominant mode is an increasing function of the drift velocity. It is interesting to note that in the collisionless case, Tsai *et al.* [19] found the peak growth rate to

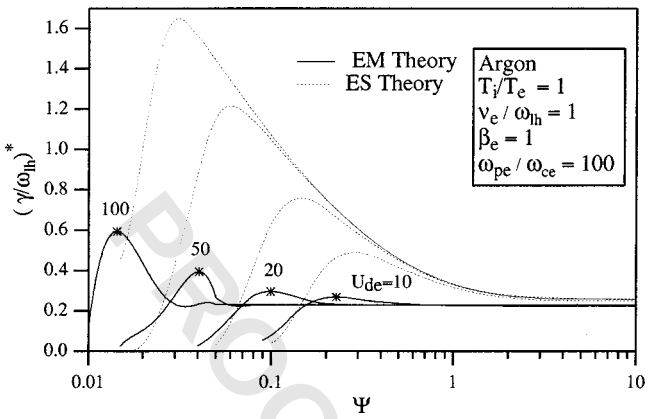

FIG. 9. Growth rates of unstable modes in argon at $\beta_e = 1$, growth maximized over wavelength as a function of the normalized propagation angle, with the dimensionless current velocity U_{de} as parameter and with the electron collision frequency set at the lower hybrid frequency. The ES theory curves are also plotted for comparison. The asterisks denote the dominant modes.

be a slowly *decreasing* function of the drift velocity. (The *increasing* trend found by Wu *et al.* [17] also for a collisionless plasma was later found by Tsai *et al.* [19] to be reversed when a proper accounting of the cyclotron harmonics is made.) This is another instance where the collisionally dominated finite-beta instability behaves more like its electrostatic counterpart than like in the collisionless and finite-beta case.

We also found that the magnitude of the drift velocity has a significant effect on the polarization of the dominant modes. In particular the calculations showed that the magnitude of $|E_s^{(1)}|^2/|E_m^{(1)}|^2$ for argon drops by two orders of magnitude at the dominant mode as U_{de} is increased from 20 to 50. This is due to the tendency of the instability to favor more oblique modes as the drift velocity increases (as in the discussion in the preceding sections) and for more oblique propagation the dominant modes have longer wavelengths that, as we have seen above, have strong electromagnetic polarization.

7. Ion mass effects

We have repeated some of the calculations above for hydrogen to provide grounds for extrapolating some of the above findings to plasma thruster operation with light propellants and to provide a connection with the space physics literature concerned with cross-field streaming instabilities. We found that the dependence of the normalized rates of the unstable modes (growth maximized over wavelength) on the mass-scaled propagation angle are almost identical to those of argon, which means that the normalized propagation angle Ψ, to the extent of the parameter range explored in this study, is a universal scaling parameter for these growth rates. The mass scaling implicit in Ψ implies that the unstable waves are spread over a substantially wider range of propagation angles for hydrogen than for argon.

The universality of Ψ as a scaling parameter is less the case for the growth-maximized frequencies and wave numbers since as the drift velocity increases they become more dependent on the ion mass. In all cases, however, we found the characteristics (frequencies, wave numbers, and growth rates) of the *dominant* modes (i.e., growth maximized over wave-length and propagation angle) to be relatively insensitive to the ion mass[2] and the trends to be largely independent of it.

V. CONCLUSIONS

The linear microstability of a cross-field-carrying plasma was studied using a dispersion relation that includes kinetic and finite-beta effects (through the complete dispersion tensor) as well as those of electron collisions (through a BGK model). The study encompassed a wide parameter range including that typical of plasmas in current-driven plasma thrusters. Comparisons were made to the better-documented cases of purely electrostatic modes ($\beta_e = 0$) or collisionless electrons ($\nu_e = 0$), allowing us to draw the following conclusions pertaining to the change in the fundamental character of the instability for the case of an equithermal plasma ($T_i/T_e \simeq 1$) in which electron collisions (referred to simply as collisions) are important ($\nu_e/\omega_{lh} \simeq 1$).

(1) Even for electron drift velocities exceeding the Alfvén velocity, finite-β_e effects are *not* globally stabilizing as previously thought, but rather result in the excitation of finite growth modes with mixed polarization even in the presence of collisions. As the electromagnetic character of the waves prevails, the role of electron collisions in destabilization becomes important.

(2) In contrast with the collisionless finite-beta results of Refs. [17,19] the polarization, at constant β_e, does not become monotonically more electrostatic as the propagation becomes more perpendicular. Also, increasing β_e shortens the wavelength of the most perpendicular modes ($\Psi > 0.3$) and lengthens that of the more oblique ones that behave more like oblique whistlers.

(3) In further contrast with its collisionless counterpart [19], the growth rate of the dominant mode is an increasing function of the drift velocity. As the drift velocity increases the instability favors more oblique modes and longer wavelengths that lead to stronger electromagnetic polarization.

(4) Contrary to the effect collisions are known to have on the dominant electrostatic modes, they can actually *increase* the growth rate of the finite-β_e dominant mode.

(5) As collisions dominate the instability changes considerably in character (from less kinetic to more fluidlike) as it reverts to more perpendicular propagation and, in many respects, behaves more like its electrostatic counterpart than like the previously studied collisionless and finite-beta instabilities.

ACKNOWLEDGMENTS

This work was supported by grants from the U.S. Air Force Office of Scientific Research and NASA-JPL.

[2]An exception must be made for the magnitude of the polarization ratio $|E_s^{(1)}|^2/|E_m^{(1)}|^2$, which is substantially lower for hydrogen even though the trend of its dependence on Ψ is the same for both atoms.

[1] D. T. Farley, J. Geophys. Res. **68**, 6083 (1963).
[2] A. Hirose and I. Alexeff, Nucl. Fusion **12**, 315 (1972).
[3] T. Maekawa and S. Tanaka, J. Phys. Soc. Jpn. **45**, 1992 (1978).
[4] J. D. Huba and S. L. Ossakow, Phys. Fluids **22**, 1349 (1979).
[5] J. D. Huba and S. L. Ossakow, J. Atmos. Terr. Phys. **43**, 775 (1981).
[6] D. Hastings and E. Niewood, J. Propul. Power **9**, 361 (1991).
[7] J. B. McBride and E. Ott, Phys. Lett. **39A**, 363 (1972).
[8] J. B. McBride, E. Ott, J. P. Boris, and J. H. Orens, Phys. Fluids **15**, 2367 (1972).
[9] A. I. Paytak and V. L. Sizonenko, Sov. Phys. Tech. Phys. **19**, 635 (1974).
[10] N. T. Gladd, Plasma Phys. **18**, 27 (1976).
[11] R. C. Davidson, N. T. Gladd, and C. S. Wu, Phys. Fluids **20**, 301 (1977).
[12] D. S. Lemons and S. P. Gary, J. Geophys. Res. **82**, 2337 (1977).
[13] J. B. Hsia *et al.*, Phys. Fluids **22**, 1737 (1979).
[14] J. D. Huba, J. F. Drake, and N. T. Gladd, Phys. Fluids **23**, 552 (1980).
[15] J. D. Huba, N. T. Gladd, and J. F. Drake, J. Geophys. Res. B **87**, 1697 (1982).
[16] Y. M. Zhou, H. K. Wong, C. S. Wu, and D. Winske, J. Geophys. Res. B **88**, 3026 (1983).
[17] C. S. Wu, Y. M. Zhou, S. T. Tsai, and S. C. Guo, Phys. Fluids **26**, 1259 (1983).
[18] J. F. Drake, J. D. Huba, and N. T. Gladd, Phys. Fluids **26**, 2247 (1983).
[19] S. T. Tsai *et al.*, Plasma Phys. Controlled Fusion **32**, 159 (1984).
[20] S. Migliuolo, J. Geophys. Res. **90**, 377 (1985).
[21] C. L. Chang, H. K. Wong, and C. S. Wu, Phys. Rev. Lett. **65**, 1104 (1990).
[22] J. D. Callen and G. E. Guest, Nucl. Fusion **13**, 87 (1973).
[23] P. L. Bhatnagar, E. P. Gross, and M. Krook, Phys. Rev. **94**, 511 (1954).
[24] E. Y. Choueiri, Phys. Plasmas **6**, 2290 (1999).
[25] P. Satyanarayana and P. K. Chaturvedi, J. Geophys. Res., [Atmos.] **90**, 12 209 (1985).
[26] E. Y. Choueiri, J. Propul. Power **14**, 744 (1998).
[27] P. Stubbe, Geophys. Res. Lett. **94**, 5303 (1989).
[28] Y. S. Dimant and R. N. Sudan, Phys. Plasmas **8**, 1411 (2001).
[29] D. L. Tilley, E. Y. Choueiri, A. J. Kelly, and R. G. Jahn, J. Propul. Power **12**, 381 (1996).
[30] E. Y. Choueiri, A. J. Kelly, and R. G. Jahn, in *Proceedings of the 22nd International Electric Propulsion Conference*, edited by ■ (■, ■, ■).
[31] E. Y. Choueiri, Phys. Plasmas **8**, 1411 (2001).
[32] O. Buneman, Phys. Rev. Lett. **10**, 285 (1963).
[33] K. Lee, C. F. Kennel, and J. M. Kindel, Radio Sci. **6**, 209 (1971).
[34] M. J. Schmidt and S. P. Gary, J. Geophys. Res. **78**, 8261 (1973).
[35] J. P. St-Maurice, J. Geophys. Res., [Atmos.] **90**, 5211 (1985).
[36] I. B. Bernstein, E. A. Frieman, M. D. Kruskal, and R. M. Kulsrud, Proc. R. Soc. London, Ser. A **244**, 17 (1958).
[37] D. S. Lemons, Ph.D. thesis, College of William and Mary, Williamsburg, VA, USA, 1977.
[38] D. W. Ross, Phys. Fluids **13**, 746 (1970).
[39] T. H. Stix, *The Theory of Plasma Waves* (McGraw Hill, New York, 1962).
[40] D. G. Swanson, *Plasma Waves* (Academic Press, San Diego, 1989).

PROOF COPY [EF8012] 013112PRE